the FEBS Journal

Methylcitrate synthase from *Aspergillus fumigatus*

Propionyl-CoA affects polyketide synthesis, growth and morphology of conidia

Claudia Maerker[1], Manfred Rohde[2], Axel A. Brakhage[3] and Matthias Brock[1,3]

1 Institute of Microbiology, University of Hannover, Germany
2 Microbial Pathogenicity, GBF Braunschweig, Braunschweig, Germany
3 Department of Molecular and Applied Microbiology, Leibniz-Institute for Natural Products Research and Infection Biology (HKI), Jena, Germany

Keywords
Aspergillus; DHN-melanin; *Galleria mellonella*; methylcitrate synthase; surface

Correspondence
M. Brock, Institute of Microbiology, University of Hannover, Herrenhäuser Str. 2, 30419 Hannover, Germany
Fax: +49 511 7625287
Tel: +49 511 76219251
E-mail: Matthias.brock@hki-jena.de

(Received 21 March 2005, revised 13 May 2005, accepted 20 May 2005)

doi:10.1111/j.1742-4658.2005.04784.x

Methylcitrate synthase is a key enzyme of the methylcitrate cycle and required for fungal propionate degradation. Propionate not only serves as a carbon source, but also acts as a food preservative (E280–283) and possesses a negative effect on polyketide synthesis. To investigate propionate metabolism from the opportunistic human pathogenic fungus *Aspergillus fumigatus*, methylcitrate synthase was purified to homogeneity and characterized. The purified enzyme displayed both, citrate and methylcitrate synthase activity and showed similar characteristics to the corresponding enzyme from *Aspergillus nidulans*. The coding region of the *A. fumigatus* enzyme was identified and a deletion strain was constructed for phenotypic analysis. The deletion resulted in an inability to grow on propionate as the sole carbon source. A strong reduction of growth rate and spore colour formation on media containing both, glucose and propionate was observed, which was coincident with an accumulation of propionyl-CoA. Similarly, the use of valine, isoleucine and methionine as nitrogen sources, which yield propionyl-CoA upon degradation, inhibited growth and polyketide production. These effects are due to a direct inhibition of the pyruvate dehydrogenase complex and blockage of polyketide synthesis by propionyl-CoA. The surface of conidia was studied by electron scanning microscopy and revealed a correlation between spore colour and ornamentation of the conidial surface. In addition, a methylcitrate synthase deletion led to an attenuation of virulence, when tested in an insect infection model and attenuation was even more pronounced, when whitish conidia from glucose/propionate medium were applied. Therefore, an impact of methylcitrate synthase in the infection process is discussed.

Propionate is the second most abundant organic acid in soil [1]. Consequently, aerobic growing soil microorganisms are supposed to be able to grow at the expense of this carbon source. The main pathways involved in propionate metabolism are that of the methylmalonyl-CoA pathway and the methylcitrate cycle. The reaction of methylmalonyl-CoA mutase leads to the citric acid cycle intermediate succinyl-CoA but is coenzyme B_{12} dependent and therefore unlikely to exist in fungi [2].

We have shown earlier that the filamentous fungus *Aspergillus nidulans* metabolizes propionate via the methylcitrate cycle [3–5]. The first key enzyme, which is specific for this cycle is the methylcitrate synthase, which catalyses the condensation of propionyl-CoA

Abbreviations
DHN, dihydroxynaphtalene; PDH, pyruvate dehydrogenase; ST, sterigmatocystin.

and oxaloacetate to methylcitrate. Methylcitrate is isomerized by a de- and rehydration step to methylisocitrate, which can be cleaved by a methylisocitrate lyase into succinate and pyruvate. Pyruvate can be used for energy metabolism and biomass formation, whereas oxaloacetate is regenerated from succinate by enzymes from the citric acid cycle.

Further investigations on *A. nidulans* showed that besides the ability to use propionate as a carbon source, the addition of propionate to glucose containing medium led to a retardation of growth, dependent on the concentration of propionate present. In addition, a methylcitrate synthase deletion strain, which is unable to remove propionyl-CoA, was inhibited even stronger than the wild type [3].

Propionyl-CoA inhibits the pyruvate dehydrogenase complex from *A. nidulans* in a competitive manner [3]. The same was shown for the complex from the bacterium *Rhodopseudomonas sphaeroides* [6] and from human liver hepatocytes [7]. Therefore, in the presence of high propionyl-CoA levels oxidation of pyruvate is disturbed, which leads to the excretion of pyruvate to the growth medium and a reduction of the growth rate. In addition to the growth inhibition caused by propionyl-CoA, also a negative effect on secondary metabolism such as polyketide synthesis was observed. Formation of sterigmatocystin (ST), a precursor of aflatoxin B1, the synthesis of ascoquinoneA, a polyketide giving the sexual ascospores the red-brown colour and synthesis of naphtopyrone, which is responsible for the colour of asexual conidia, were all impaired in the presence of accumulated propionyl-CoA [3,8,9]. ST and ascoquinoneA are formed in the late stage of vegetative growth (> 70 h), whereas naphtopyrone formation starts within the first 24 h. In a methylcitrate synthase deletion strain a strong reduction of ST and ascoquinoneA was observed even in the absence of propionate, which can be explained by the accumulation of propionyl-CoA from amino acid degradation (valine, isoleucine and methionine) at conditions of carbon starvation. In contrast, inhibition of naphtopyrone synthesis was only observed when propionate was added to the growth medium. In the early growth phase on glucose no significant accumulation of propionyl-CoA occurred but the levels increased dramatically upon the addition of propionate. Therefore the conclusion was reached that in *A. nidulans* the ratio between acetyl-CoA and propionyl-CoA had to be > 1 for an undisturbed polyketide synthesis [3,8].

Aspergillus fumigatus is an opportunistic human pathogen, which can cause different diseases, among them invasive aspergillosis, which predominantly occurs in immunocompromised patients. Infection generally starts with inhalation of conidia, which are ubiquitous in the environment. Because of the small size of conidia (< 3 μm in diameter) they can reach the alveoli of the lung and, in case of a suppressed immune system, start to germinate. Once escaped the alveolar macrophages and the granulocytes the fungus can reach the blood stream and becomes distributed over the whole body, leading to the infection of other organs. This stage of infection is accompanied with a very high mortality rate ($\approx 90\%$), despite treatment with antifungals such as amphotericin B and itraconazol, which have severe side-effects [10–13].

In order to identify new targets for drug development and to understand the impact of specific fungal genes in virulence, several mutants of *A. fumigatus* had been constructed and checked for their attenuation in virulence in a murine infection model. Among others, especially mutants, which displayed defects in central metabolic functions such as the cAMP network, iron assimilation and amino acid biosynthesis exhibited an attenuation in virulence [14–17]. In addition, mutants with a defective gene coding for a polyketide synthase (*pks*P) were identified and checked for virulence in different models. *pks*P mutants are unable to produce the dihydroxynaphtalene-melanin (DHN-melanin). The main content of this melanin is found within the conidia, giving them their grey-green colour, which reasons, why a mutation of the *pks*P gene leads to white conidia [18,19]. These conidia showed a strongly reduced ability to survive within activated human monocyte derived macrophages and an attenuated ability to cause an invasive aspergillosis in a murine infection model [20–22]. This effect might be due to the importance of DHN-melanin to scavenge reactive oxygen species produced during the immune defence. In addition, DHN-melanin seems to be required for binding of proteins to the surface of conidia. The conidial surface of *A. fumigatus* is completely covered with a highly organized layer of proteins, especially hydrophobins [23]. In contrast to that conidia of a *pks*P mutant show a plain surface with hardly any attached proteins [18,19]. Therefore, a role of DHN-melanin in organization of surface proteins can be assumed.

In this study we purified and characterized the methylcitrate synthase from *A. fumigatus* and deleted the corresponding gene. The growth behaviour at different carbon sources as well as the effect of propionate on spore colour formation and structure of the conidial surface from mutant and wild-type strain was investigated and compared to mutants from *A. nidulans*. Furthermore, an insect infection model was used to analyse a possible attenuation in virulence of a methylcitrate synthase deletion strain.

Results

Purification and biochemical characterization of methylcitrate synthase

Methylcitrate synthase (EC 2.3.3.5), a key enzyme of propionate degradation via the methylcitrate cycle, was identified from crude extracts of propionate grown mycelium. Starting from 3.3 g of mycelium the protein was purified from a specific activity of 0.13 $U \cdot mg^{-1}$ in crude extracts 136-fold to 17.7 $U \cdot mg^{-1}$ (turnover number 14.2 s^{-1} for one monomer) and a yield of 17% (Table 1). The resulting protein revealed a single major band with a mass of around 45 kDa (Fig. 1A), which is similar to that of the purified protein from *A. nidulans* (Fig. 1B) (see also [5]). In addition to methylcitrate synthase activity, the purified protein also displayed significant citrate synthase activity with a specific activity of 48 $U \cdot mg^{-1}$ (turnover number 38.6 s^{-1} for one monomer). This citrate synthase activity is distinct from that of the citrate synthase from the tricarboxylic acid cycle (EC 2.3.3.1), because a methylcitrate synthase deletion mutant (see below) still displayed citrate synthase activity and showed no visible growth defect on glucose or acetate as sole carbon sources. Therefore, we will further refer to the purified protein as methylcitrate synthase, because that seems to be the main feature of the enzyme.

Further characterization of the biochemical properties revealed similar pH- and temperature dependencies, K_m-values and catalytic efficiencies for the different substrates as determined for methylcitrate synthase from *A. nidulans* (for comparison see Table 2). In addition, the enzyme was stable for at least 3 h at a pH between 5.0 and 9.0 and a temperature of up to 40 °C. At 60 °C the half-life of enzymatic activity was 11 min.

Sequence identification and analysis

The N-terminal sequence of the purified methylcitrate synthase was determined by Edman-degradation and revealed the following peptide sequence: STAEPDLKTALKAVIPAKRELFKQVKE. This sequence

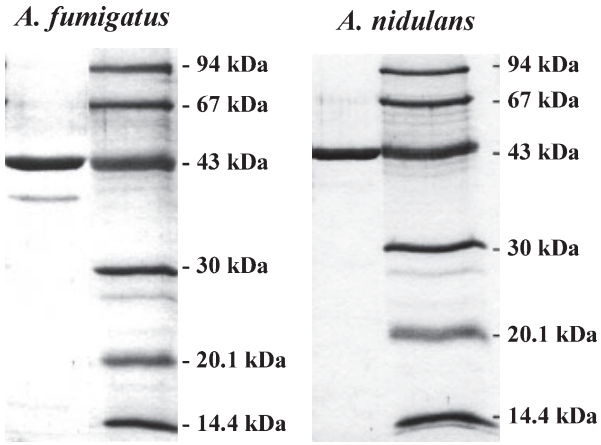

Fig. 1. SDS/PAGE of purified methylcitrate synthase from *A. fumigatus* and *A. nidulans*. Three micrograms of the purified proteins were loaded.

was compared to the sequence of the methylcitrate synthase from *A. nidulans* [5] and displayed an identity of 74% over the analysed region. Therefore, the protein sequence of the methylcitrate synthase from *A. nidulans* (Accession No. CAB53336) was used as a template for a BLAST-search against the unfinished genome of *A. fumigatus* at TIGR. A sequence with an identity of > 80% was identified at contig 4899 (position 501421–502956). In order to obtain the sequence of the coding region, cDNA was produced and sequenced (Accession No. AJ888885). Comparison of genomic and cDNA revealed two introns with a size of 58 and 64 bp. Removal of the introns led to an open reading frame of 465 amino acids and a molecular mass of 51.41 kDa, which is somewhat higher than 45 kDa determined by SDS/PAGE. Analysis of the protein sequence by the programs PSORT and MITOPROT revealed an N-terminal leader peptide reaching to position 28. This peptide is cleaved off during mitochondrial import and lowers the molecular mass to 48.21 kDa, which is in good agreement with that observed from the polyacrylamide gel. The cleavage of the signalling peptide furthermore explains, why the serine at

Table 1. Purification record of methylcitrate synthase from *A. fumigatus* ATCC46654 grown on propionate as sole carbon source. Activity was determined with propionyl-CoA and oxaloacetate as substrates.

Purification step	Protein (mg)	Units ($\mu mol \cdot min^{-1}$)	Specific activity ($U \cdot mg^{-1}$)	Purification factor	Yield
Crude extract	140	18.1	0.13	1	100%
90% $(NH_4)_2SO_4$-precipitate	18.4	12.0	0.65	5	66%
Phenyl sepharose	1.17	5.0	4.27	33	28%
Hydroxyapatite	0.17	3.1	17.7	136	17%

Table 2. Comparison of properties of methylcitrate synthases from *A. fumigatus* and *A. nidulans*.

Parameter	McsA *A. fumigatus*	McsA *A. nidulans*
Specific activity (propionyl-CoA)	17.7 U·mg^{-1}	14.5 U·mg^{-1}
Specific activity (acetyl-CoA)	48.0 U·mg^{-1}	41.5 U·mg^{-1}
K_m Propionyl-CoA	1.9 μM	1.7 μM
K_m Acetyl-CoA	2.6 μM	2.5 μM
K_m Oxaloacetate	2.7 μM	0.6 μM
Catalytic efficiency (propionyl-CoA)	7.5×10^6 s^{-1}·M^{-1}	6.5×10^6 s^{-1}·M^{-1}
Catalytic efficiency (acetyl-CoA)	1.4×10^7 s^{-1}·M^{-1}	1.2×10^7 s^{-1}·M^{-1}
Maximum activity (pH-range)	8.0–9.0	8.5–9.5
Maximum activity (temperature-range)	50–60 °C	45–52 °C
Molecular mass/no. of amino acids	51.41 kDa/465	50.58 kDa/460
Leader peptide for mitochondrial import	First 28 aa	First 24 aa
Molecular mass (native)/no. of amino acids	48.21 kDa/437	47.93 kDa/436
pI of protein (with/without leader-peptide)	8.95/6.93	8.93/7.25
Number and length of introns	2 introns; 58 and 64 bp	2 introns; 95 and 49 bp

position 29 was determined as the first amino acid appearing from N-terminal sequencing. The overall identity of the methylcitrate synthases from *A. nidulans* and *A. fumigatus* was 88%.

Identification of methylcitrate synthase mutants

The *pyrG* gene from *A. nidulans* was used to replace the coding region of methylcitrate synthase of the uracil auxotrophic *A. fumigatus* strain CEA17. The *pyrG* gene from *A. nidulans* was tested to be functional in *A. fumigatus* and a CEA17 strain transformed only with this gene was uracil prototroph and displayed no growth defects, when compared to the wild-type ATCC46645.

Strains, which were transformed with the deletion construct, were checked by Southern analysis with two probes. One probe consisted of the *pyrG* gene from *A. nidulans* and a second probe of the upstream region of the *mcsA* gene (Fig. 2). All clones, which showed a site-specific integration, were unable to grow on propionate as sole carbon and energy source. The use of glucose, glycerol, ethanol or acetate as sole carbon and energy source displayed no growth defects. Therefore, the deleted gene is essential only for propionate metabolism.

Phenotypic characterization of methylcitrate synthase mutants on mixed carbon sources

The effect of propionate in combination with other carbon sources on growth of a methylcitrate synthase deletion mutant and a wild-type strain was investigated in liquid cultures. The inhibitory effect of propionate in combination with glucose was tested by use of 50 mM glucose as main carbon source and addition of different amounts of propionate. After incubation of replicate cultures for 20 h at 37 °C the mycelium was harvested, dried and weighed. The deviation of the independent cultures was always less than 5%. Growth on glucose as sole carbon source was taken as 100%. A similar approach was made for determination of growth inhibition when acetate was the main carbon source, except that the growth time was prolonged to 44 h and acetate (50 mM) as sole carbon source was taken as 100%. An overview about the inhibition rates is given in Table 3. As expected from earlier studies on *A. nidulans* the methylcitrate synthase mutant was inhibited much stronger on glucose/propionate medium than the wild type. However, it is noteworthy that both, *A. fumigatus* wild type and the mutant strain were more sensitive against propionate than their *A. nidulans* counterparts (for comparison: *A. nidulans* wild type grown for 26 h on 50 mM glucose + 50 mM propionate yielded 60% residual biomass, the deletion strain produced 48% at these conditions).

To proof the assumption that growth inhibition might be due to an inhibition of the pyruvate dehydrogenase complex, pyruvate excretion into the growth medium was tested. Especially the *ΔmcsA*-strain excreted high amounts of pyruvate, dependent on the concentration of propionate present. Some pyruvate excretion was also observed with the wild type, but levels were approximately fivefold lower (Table 3). Additionally, excretion of pyruvate of an *A. fumigatus ΔmcsA*-strain is much higher than that of a methylcitrate synthase mutant from *A. nidulans*. Growth of the latter for 72 h on medium containing 50 mM glucose and 100 mM propionate yielded 2.21 mmol pyruvate·g dried mycelium^{-1} [3]. The same amount of pyruvate was found, when the former strain (*A. fumigatus*) was

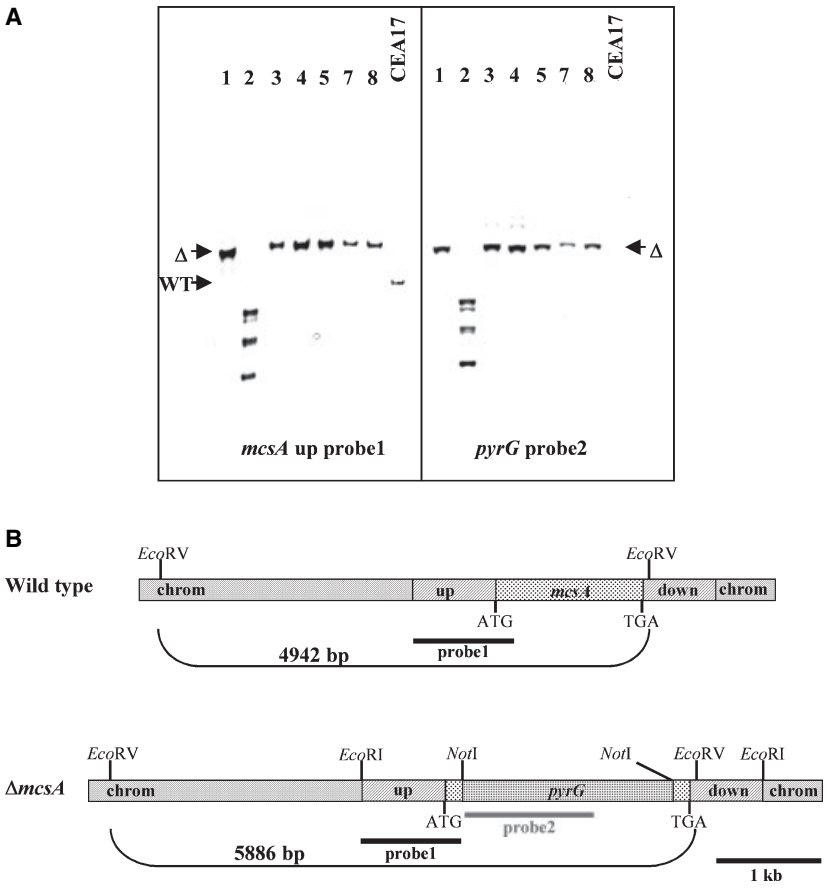

Fig. 2. Deletion of the methylcitrate synthase (*mcsA*) from *A. fumigatus*. (A) Southern blots with probe1 against the upstream region of the *mcsA* gene and probe2 against the *pyrG* gene from *A. nidulans*. (B) Schematic drawing of the genomic situation of the wild type and a methylcitrate synthase deletion strain.

grown for 20 h on medium containing 50 mM glucose and 20 mM propionate (Table 3).

When acetate was used as main carbon source the wild-type strain was not negatively affected by the addition of propionate, whereas in the presence of 50 mM propionate a 45% reduction of biomass formation was observed with the methylcitrate synthase mutant. This inhibitory effect is much weaker than that observed on glucose and furthermore, only small amounts of pyruvate were found in the growth medium. Despite some accumulation of propionyl-CoA, acetate was shown to compete with propionate for activation. Additionally, the pyruvate dehydrogenase complex (see below) is not required on acetate [24] and was shown to be a major target for growth inhibition in *A. nidulans* [3].

Effect of propionyl-CoA on the pyruvate dehydrogenase complex

The pyruvate dehydrogenase complex (PDH complex; EC 1.2.4.1) is essential for growth on glucose and propionate but not on acetate [3]. Pyruvate is converted to acetyl-CoA via the PDH complex and inserted into the citric acid cycle. PDH complexes are competitively inhibited by high acetyl-CoA/CoASH ratios, trapping the complex in its acetylated form [25]. It was shown earlier in *A. nidulans* that not only acetyl-CoA but also propionyl-CoA can act as a competitive inhibitor with respect to the CoASH binding site with an K_i of 50 μM [3]. Therefore, we investigated the inhibitory effect of propionyl-CoA in competition to CoASH-binding on the PDH complex from *A. fumigatus*. The K_m-value for CoASH increased in the presence of 0.15 mM propionyl-CoA from 8.5 μM to 32.5 μM. This leads to a calculated K_i of 53 μM, which is similar to that from *A. nidulans* and explains the excretion of pyruvate during growth on glucose/propionate medium. Therefore, the PDH complex is a target for both, growth inhibition and pyruvate excretion, but this inhibition is not sufficient to explain the increased sensitivity of *A. fumigatus* towards propionate compared to *A. nidulans*.

Intracellular acetyl-CoA and propionyl-CoA content

In order to proof, whether propionyl-CoA accumulates under certain growth conditions, the wild-type ATCC46645 and the methylcitrate synthase mutant

Table 3. Growth inhibition and pyruvate excretion of a methylcitrate synthase mutant and the wild-type ATCC46645 by addition of propionate. Glucose and acetate concentrations were always 50 mM. Propionate concentrations were in mM and given by numbers. Pyruvate excretion is calculated for 1 g of dried mycelium.

Carbon source	Wild type	*ΔmcsA*
	Relative growth (%)	Relative growth (%)
Growth time: 21 h		
Glucose	100	100
Glucose/Propionate 10	77 ± 2	22 ± 3
Glucose/Propionate 20	59 ± 3	16 ± 2
Glucose/Propionate 50	35 ± 6	8 ± 2
Growth time 44 h		
Acetate	100	100
Acetate/Propionate 10	102 ± 2	85 ± 4
Acetate/Propionate 20	105 ± 4	75 ± 4
Acetate/Propionate 50	101 ± 2	55 ± 5
	Pyruvate ($\mu mol \cdot g^{-1}$)	Pyruvate ($\mu mol \cdot g^{-1}$)
Growth time 20 h		
Glucose	187 ± 20	250 ± 30
Glucose/Propionate 10	254 ± 24	1346 ± 61
Glucose/Propionate 20	317 ± 25	2168 ± 25
Glucose/Propionate 50	490 ± 30	2724 ± 98
Growth time 44 h		
Acetate	23 ± 4	35 ± 4
Acetate/Propionate 10	31 ± 3	41 ± 5
Acetate/Propionate 20	37 ± 4	56 ± 4
Acetate/Propionate 50	75 ± 8	98 ± 7

were analysed for their acyl-CoA content. Mycelium was harvested from glucose (50 mM) medium after 20 h, glucose (50 mM)/propionate (20 mM) medium after 32 h and glucose (50 mM)/acetate (50 mM)/propionate (20 mM) medium after 32 h. Due to the strong growth inhibition of the mutant in the presence of propionate (see Table 3) a maximum of 20 mM propionate was used. Acyl-CoA was extracted and concentrations of acetyl-CoA were measured with citrate synthase, whereas propionyl-CoA was determined with methylcitrate synthase. The total values were correlated to the mycelial dry weight. Two independent mycelia from each growth condition were investigated. Total amounts slightly differed between each pair, which is most likely due to a different degree of disruption of the mycelium and some loss of the acyl-CoA during the purification procedure. Anyhow, an approval of the procedure with known concentrations of acetyl-CoA and propionyl-CoA showed that both thioesters were lost to the same extend [3]. This is furthermore assisted by the observation that the ratios of acetyl-CoA and propionyl-CoA remained almost constant. The results from one determination are given in Table 4.

As expected, only tiny amounts of propionyl-CoA were found, when cells were grown on glucose as sole carbon source and the amount of acetyl-CoA was much higher than that of propionyl-CoA. The addition of propionate to glucose medium strongly increased the propionyl-CoA content, especially in the methylcitrate synthase mutant, where significantly higher concentrations of propionyl-CoA than acetyl-CoA were found. In the wild-type strain also some increase in propionyl-CoA was observed, but it never exceeded the value of acetyl-CoA, implicating that a functional methylcitrate synthase can efficiently remove propionyl-CoA. The addition of acetate to glucose/propionate medium lowered the amount of propionyl-CoA in both strains. This indicates that some competition of acetate with propionate exists, which can either originate from an inhibition of propionate uptake or from a competition for the activation to the corresponding CoA-ester. Despite this effect of acetate, some increase of propionyl-CoA was still observed with the mutant and the ratio of both thioesters was nearly 1 : 1, which indicates that propionate is still activated, although the concentration of acetate was 2.5-fold higher than that of propionate.

Table 4. Acetyl-CoA and propionyl-CoA concentrations from the methylcitrate synthase mutant (*ΔmcsA*) and the wild type (WT). Strains were grown on different carbon sources for the indicated times. Amounts of acyl-CoA (in nmol) were calculated for 1 g of dried mycelium. Concentrations of the corresponding carbon sources (mM) are given in brackets. Gluc, glucose; Prop, propionate; Ac, acetate; Ac-CoA, acetyl-CoA; Prop-CoA, propionyl-CoA.

Carbon source and growth time	*ΔmcsA* Ac-CoA	*ΔmcsA* Prop-CoA	Ratio Ac-CoA/Prop-CoA	WT Ac-CoA	WT Prop-CoA	Ratio Ac-CoA/Prop-CoA
Gluc (50) 20 h	38.4	6.0	6.4 : 1	36.5	8	4.6 : 1
Gluc (50)/Prop (20) 32 h	31.9	97.3	1 : 3	30.4	25.6	1.2 : 1
Gluc (50)/Prop (20)/Ac (50) 32 h	17.9	14.4	1.2 : 1	16.0	6.0	2.7 : 1

Table 5. Specific acetyl-CoA synthetase (Acs) and propionyl-CoA synthetase (Pcs) activities from *A. fumigatus* (ATCC46645) and *A. nidulans* wild type (A26). Both strains were grown on indicated carbon sources (Gluc, glucose; Prop, propionate; Ac, acetate; numbers denote concentrations of carbon sources in mM). After complete glucose consumption, cells were incubated for further 12 h.

Carbon source (conc. in mM)	*A. fumigatus* Acs ($mU \cdot mg^{-1}$)	*A. fumigatus* Pcs ($mU \cdot mg^{-1}$)	*A. nidulans* Acs ($mU \cdot mg^{-1}$)	*A. nidulans* Pcs ($mU \cdot mg^{-1}$)
Gluc 50/Prop 100	13	15	22	10
Prop 100[a]	49	56	133	77
Ac 100	56	40	135	59
Ac 100/Prop 100	41	32	153	58

[a] Cells were grown in the presence of 10 mM glucose.

Activation of acetate and propionate to the corresponding CoA-esters

Methylcitrate synthase and PDH complex from *A. nidulans* and *A. fumigatus* display very similar biophysical characteristics. Nevertheless, an *A. fumigatus ΔmcsA*-strain is stronger inhibited in growth and excretes more pyruvate than an *A. nidulans ΔmcsA*-strain, when grown under comparable conditions.

In *A. nidulans* the activation of acetate and propionate to the corresponding CoA-esters is performed by at least two enzymes. One is the acetyl-CoA synthetase (EC 6.2.1.1), which possesses a high specificity for acetate but also activates propionate with a 47-fold lower efficiency. A second enzyme possesses a 14-fold higher efficiency for propionate as a substrate and was clearly identified from an acetyl-CoA synthetase mutant. This enzyme is specifically produced in the presence of propionate and is therefore unable to support growth on acetate as sole carbon source. Additionally, in a wild-type situation of *A. nidulans*, where both activating enzymes are intact, acetate is always the preferred substrate over propionate [3].

In order to investigate the activation of acetate and propionate in *A. fumigatus*, activities of the wild-type strain were investigated, when grown on different carbon sources. Mean values from two independent determinations of both specific activities in comparison to that from an *A. nidulans* wild-type strain [3] are given in Table 5.

In comparison to *A. nidulans*, the overall activity for the activation of acetate is always significantly lower in *A. fumigatus*. Additionally, the propionyl-CoA synthetase activity (EC 6.2.1.17) in *A. fumigatus* exceeds that of acetyl-CoA synthetase, when no acetate is present. These data indicate that *A. fumigatus* also possesses, besides an acetyl-CoA synthetase, a specific propionyl-CoA synthetase, which is induced by propionate and may count for the increased sensitivity of *A. fumigatus* towards propionate. A determination of the K_m-values for the substrates acetate and propionate was performed to proof that both activities derive from different enzymes. Crude extracts of acetate grown mycelium showed a K_m with acetate of 34.1 μM and with propionate of 865 μM. In contrast, the K_m with acetate was 85.1 μM and with propionate 96 μM, when mycelium was grown on propionate. That gives the evidence that at least two different enzymes were involved in the activation of the acylates to the CoA-esters. Nevertheless, in order to access an activity and a K_m to one specific enzyme, mutants have to be constructed, which only possess one of both enzymes.

Effect of propionate on spore colour formation, surface of conidia and H_2O_2 sensitivity

Methylcitrate synthase mutants of *A. nidulans* are severely affected in polyketide synthesis upon the accumulation of propionyl-CoA [3,8]. The inhibition of naphtopyrone synthesis, the polyketide responsible for the spore colour of *A. nidulans* [26], can be visualized by the reduced formation of spore colour, when grown in the presence of propionate.

In *A. fumigatus* spore colour also derives from a polyketide, the dihydroxynaphtalene-melanin (DHN-melanin), which is produced by the polyketide synthase PksP. Mutants, which carry a defective or deleted *pks*P gene carry completely white spores [18,19]. The *pksP* gene was shown to play an important role in the establishment of invasive aspergillosis in a murine infection model. Furthermore, spores of a *pksP* mutant, which are white, were more sensitive against the attack by human monocyte derived macrophages and H_2O_2 [20]. Therefore, we were interested, whether an accumulation of propionyl-CoA can lead to a reduction of the DHN-melanin level in *A. fumigatus*. Conidia of a wild-type strain, of a methylcitrate synthase mutant and of a *pks*P mutant were point inoculated on agar plates containing solely glucose or glucose with propionate (10 mM) as carbon sources. As shown in Fig. 3A the

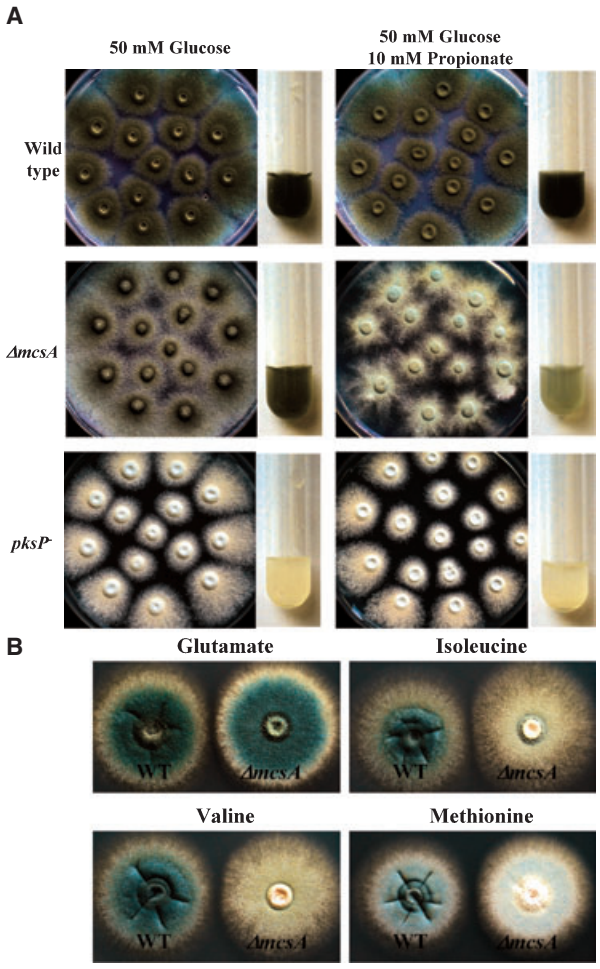

Fig. 3. Spore colour of different *A. fumigatus* strains upon the addition of propionate and amino acids. (A) Wild type, *mcsA* deletion strain and *pksP* mutant strain grown in the presence and absence of 10 mM propionate for 6 days at 37 °C. Spore suspensions are shown on the left site of the corresponding plates and contain 3×10^8 conidia·mL^{-1} each. (B) Wild type and *mcsA* deletion strain grown in the presence of propionyl-CoA generating amino acids or glutamate (as a control).

ΔmcsA-strain was strongly affected in spore colour formation in the presence of propionate. However, even in the absence of propionate some reduction in spore colour, especially at the outer areas of central colonies, was observed. Starvation, caused by complete consumption of glucose leads to the internal degradation of amino acids and an accumulation of propionyl-CoA as shown for *A. nidulans* [8]. Therefore, some accumulation of propionyl-CoA may also occur on glucose medium in the mutant strain and affect the synthesis of polyketides. Nevertheless, glucose-grown colonies carry stronger coloured conidia than colonies grown in the presence of propionate. In contrast, the wild-type strain is hardly affected in spore colour formation in the presence of 10 mM propionate. This indicates that propionyl-CoA indeed is a potential inhibitor of polyketide synthesis in *A. fumigatus*.

The use of the amino acids methionine, isoleucine and valine had a similar effect on spore colour formation of the methylcitrate synthase deletion strain. Supplementation of agar plates with these amino acids strongly reduced the colour of the conidia, whereas the wild-type strain was hardly affected. The amino acid glutamate, which was used as a control did not affect polyketide synthesis (Fig. 3B). This proofs that the former amino acids were degraded to propionyl-CoA, which cannot be further metabolized in the mutant strain. Furthermore, a replacement of nitrate as nitrogen source by one of the above mentioned propionyl-CoA generating amino acids hardly permitted growth of the mutant strain, whereas some residual growth was observed with the wild type (data not shown).

We were further interested in the appearance of the conidial surface. The conidia of the wild type show a strong ornamentation, which derives from several thick layers of proteins surrounding the conidia. A large impact is given to hydrophobins, which seem to protect the conidia from the environment and may play a role in the resistance against killing by alveolar macrophages [23,27,28]. In contrast to that the white conidia of a *pks*P mutant strain posses a plain surface and seem to be disordered in the orientation of surrounding proteins. Figure 4 shows scanning electron micrographs of conidia from wild type, *ΔmcsA* and *pksP* mutant strains grown on glucose and glucose/propionate (10 mM) minimal medium. The wild-type and *ΔmcsA* conidia showed the expected ornamentation of the conidial surface when harvested from glucose minimal medium. By contrast, a smooth surface became visible in case of the *pksP* mutant regardless of the carbon sources the spores derived from. Interestingly, the wild type slightly altered the appearance of the surface of conidia in the presence of propionate even though the conidia were strongly coloured. However, ornamentation did not change further even upon the addition of 50 mM propionate (data not shown). In case of the *ΔmcsA*-strain the effect on the conidial surface was more pronounced. In the presence of propionate, some spores showed a surface as smooth as the *pksP* mutant strain, whereas others still displayed a rough surface. That shows that propionate and the associated accumulation of propionyl-CoA has a stronger effect on the appearance of the conidial surface from a methylcitrate synthase deletion strain than on that of the wild type.

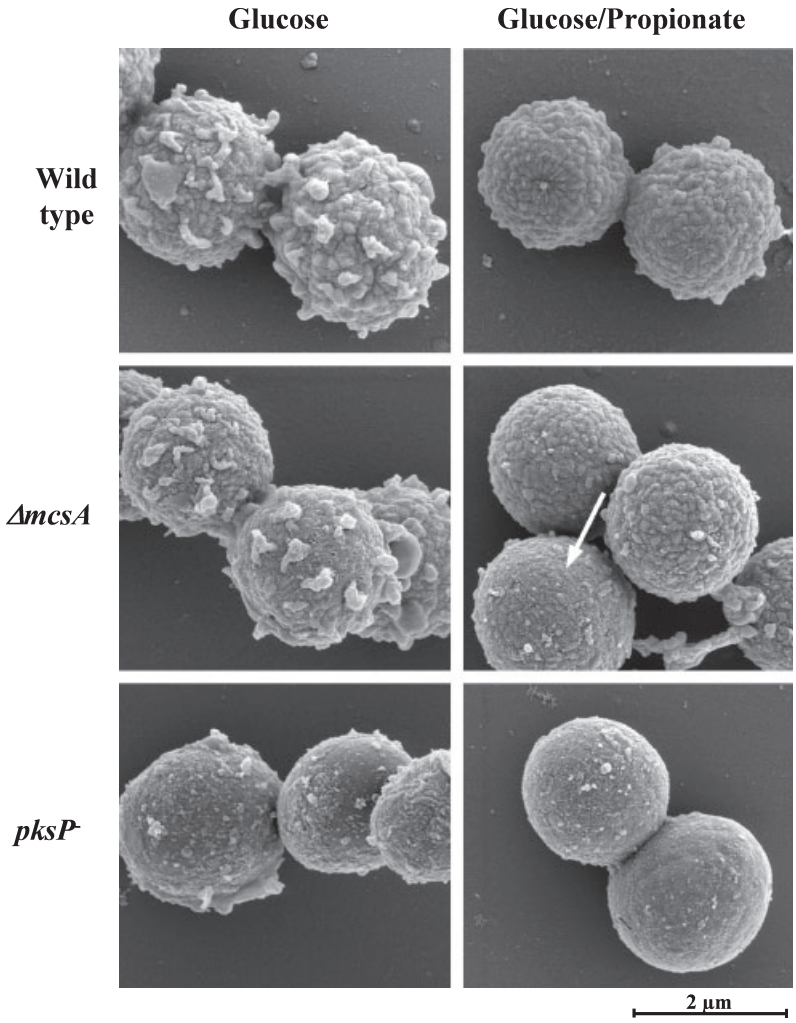

Fig. 4. Field emission scanning electron micrographs of conidia from different *A. fumigatus* strains and growth conditions. Wild type = ATCC46645, *ΔmcsA* = methylcitrate synthase deletion strain, *pksP*$^-$ = strain with a mutation in the polyketide synthase gene *pksP*. The arrow denotes a conidium with strongly reduced surface ornamentation.

In order to investigate, whether this altered conidial surface effects the sensitivity against H_2O_2, conidia from the conditions described above were exposed to different H_2O_2-concentrations in plate diffusion assays. The inhibition zones obtained with the conidia from the two different carbon sources were compared and are shown in Table 6. Both, wild type and *ΔmcsA* showed an increase in the diameter of the inhibition zone, when conidia derived from glucose/propionate medium, but the effect was stronger in case of the *ΔmcsA* strain than that on the wild type. In contrast, inhibition zones of the *pksP* mutant strain were not dependent on the carbon source, from where the spores derived. Nevertheless, as expected, the inhibition zones of the *pksP* mutant were always largest, followed by *ΔmcsA* (glucose/propionate) and wild type (glucose/propionate). These results imply that melanin content and appearance of the conidial surface are linked and relevant for the resistance against reactive oxygen species.

Virulence studies in an insect infection model using larvae of *Galleria mellonella*

Insects are quite often used as a model to study attenuation of virulence of pathogenic microorganisms. Especially strains of *Candida albicans* and *Pseudomonas aeroginosa* have been tested in this model [29–33]. Interestingly, a significant number of mutant strains behaved very similar in the insect model when compared to a murine infection model and revealed, e.g. that clinical isolates were more pathogenic than laboratory isolates. The model was also used to investigate the virulence of different *Aspergillus* strains with respect to gliotoxin production and kill of larvae [34]. Therefore, this insect model helps to evaluate, whether a mutant strain might display an attenuated virulence before using the mouse model.

We used larvae of *Galleria mellonella*, which were infected with conidia from *A. fumigatus* wild-type ATCC46645 as one control and as a second control

Table 6. Sensitivity of wild-type, *pksP*⁻ and *ΔmcsA* conidia against different amounts of a 3% H_2O_2 solution. Conidia derived either from minimal medium with 50 mM glucose (G50) or 50 mM glucose +10 mM propionate (G50/P10). The mean value of the diameter of inhibition zones and the deviation of three independent zones is given. *Δ* from mean gives the difference of the inhibition zones of a single strain from the two carbon sources.

Amount H_2O_2	Strain	Growth medium	Inhibition zone (mm)	*Δ* from mean (mm)
50 μL	*pksP*⁻	G50	3.38 ± 0.02	
50 μL	*pksP*⁻	G50/P10	3.38 ± 0.03	0
50 μL	Wild type	G50	2.82 ± 0.03	
50 μL	Wild type	G50/P10	2.90 ± 0.02	0.08
50 μL	*ΔmcsA*	G50	2.75 ± 0.03	
50 μL	*ΔmcsA*	G50/P10	2.95 ± 0.02	0.20
75 μL	*pksP*⁻	G50	3.63 ± 0.03	
75 μL	*pksP*⁻	G50/P10	3.60 ± 0	−0.03
75 μL	Wild type	G50	3.00 ± 0.05	
75 μL	Wild type	G50/P10	3.12 ± 0.02	0.12
75 μL	*ΔmcsA*	G50	2.90 ± 0.05	
75 μL	*ΔmcsA*	G50/P10	3.12 ± 0.02	0.22
100 μL	*pksP*⁻	G50	3.77 ± 0.03	
100 μL	*pksP*⁻	G50/P10	3.80 ± 0.03	0.03
100 μL	Wild type	G50	3.15 ± 0.05	
100 μL	Wild type	G50/P10	3.25 ± 0	0.10
100 μL	*ΔmcsA*	G50	3.05 ± 0.05	
100 μL	*ΔmcsA*	G50/P10	3.30 ± 0.05	0.25

the *pksP* mutant, which only produces white spores. In order to gain differently coloured conidia (Fig. 3A) of the methylcitrate synthase deletion strain, spores were harvested from media either with or without the addition of 10 mM propionate. Larvae were infected as described in the experimental procedures and observed for 6 days for their survival. As depicted in Fig. 5, 50% of the larvae infected with wild-type spores had died at the end of the experiment. A higher survival rate was observed in case of the *pksP* mutant, which is in agreement with earlier investigations in the murine and macrophage model [20]. An attenuated virulence was also observed, when conidia from the *ΔmcsA*-strain were used, which was even more pronounced, when the conidia derived from medium containing propionate. Therefore we conclude that both, the morphology of the conidia and the methylcitrate synthase posses an impact on virulence in this insect model and might also be important in the establishment of an invasive aspergillosis in a murine model.

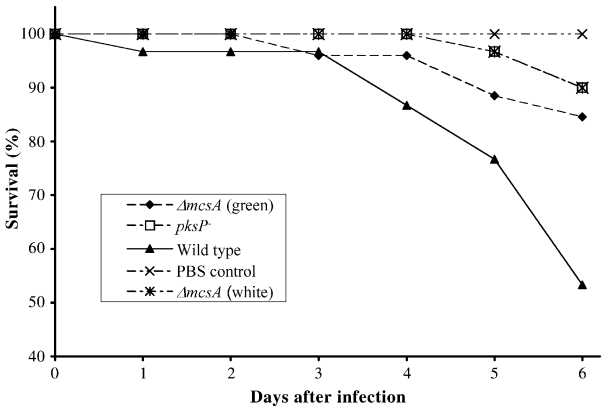

Fig. 5. Survival of *Galleria mellonella* larvae after infection with conidia from *A. fumigatus* wild type, methylcitrate synthase deletion strain (*ΔmcsA*; glucose and glucose/propionate harvested spores) and from the *pksP* mutant (*pksP*⁻). Larvae were infected with 5×10^6 spores, incubated in the dark at 22 °C and monitored for 6 days. Larvae inoculated with NaCl/P_i served as a control. (Note that the graphs of *pksP*⁻ and '*ΔmcsA* white' are overlapping.)

Discussion

A. fumigatus metabolizes propionate via the methylcitrate cycle. The biochemical properties of methylcitrate synthase from *A. fumigatus* are very similar to that from *A. nidulans*. In addition, both enzymes share an 88% amino acid identity over the whole sequence. Additional sequences for putative methylcitrate synthases can be obtained, when fungal databases are searched (Table 7). The identity of the *A. fumigatus*

Table 7. Comparison of some characteristics of methylcitrate synthase from *A. fumigatus* to (hypothetical) methylcitrate synthases from other fungal sources. Probability defines the calculated likelihood for mitochondrial import as predicted by the program MITOPROT.

Source of sequence	Accession	No. of amino acids	Identity against *A. fumigatus*	Signal cleavage (position)	Cleaved sequence	Probability (max = 1.0)
A. fumigatus	CAI61947	465	100%	29	..RGY/ST	0.9861
A. nidulans	CAB53336	460	88%	24	..RGY/AT	0.9914
N. crassa	XP_331681	470	70%	28	..RGY/AT	0.9859
G. zea	EAA67271	472	70%	30	..RGY/AT	0.9936
M. grisea	EAA47374	458	69%	14	..RNY/SA	0.5262
Y. lipolytica	CAG78959	459	60%	23	..KRF/AS	0.9865
U. maydis	EAK82252	474	53%	32	..VRF/AS	0.9524
S. cerevisiae	NP_014398	479	51%	38	..RHY/SS	0.9607

methylcitrate synthase to proteins from filamentous fungi such as *A. nidulans*, *Neurospora crassa*, *Giberella zea* and *Magnaporthe grisea* is in the range from 70 to 90%, whereas sequences from the yeast-like fungi *Yarrowia lipolytica*, *Ustilago maydis* and *Saccharomyces cerevisiae* display an identity of 50–60%. Additionally, all proteins contain a mitochondrial signal peptide and are distinct from the citric acid cycle citrate synthase. Due to the indispensable role of methylcitrate synthases in propionate degradation and the identification of putative methylcitrate synthases from several sequenced fungal genomes it is implied that the methylcitrate cycle may be the general pathway for the degradation of propionate in fungi.

A deletion of the genomic region coding for methylcitrate synthase leads to an inability to use propionate as a substrate for growth. Nevertheless, propionate can still become activated to propionyl-CoA and accumulates in the mutant strain. The phenotypic effects caused by propionyl-CoA are similar to that observed for a methylcitrate synthase deletion strain from *A. nidulans*. Mutants are much more sensitive towards the addition of propionate to glucose containing medium than the wild type and in addition, the formation of polyketides is disturbed [3,5,8,9]. Therefore, methylcitrate synthase plays a key role in the removal of propionyl-CoA. This is consistent with the low K_m-value for the substrates propionyl-CoA and oxaloacetate and the hydrolysis of the thioester bond, which makes the reaction irreversible under physiological conditions.

Interestingly, *A. fumigatus* is more sensitive against propionate in the presence of glucose than *A. nidulans*, which is true for the wild type and the methylcitrate synthase mutant. Furthermore, in *A. nidulans* the addition of acetate to glucose/propionate medium had a beneficial effect on growth and polyketide synthesis, which is much less pronounced in case of *A. fumigatus*. The propionyl-CoA levels in *A. nidulans* dropped below that of acetyl-CoA, when equal amounts of acetate and propionate were added, not only for the wild type but also for the methylcitrate synthase mutant. In *A. fumigatus* much higher concentration of acetate than that of propionate are required to lower the level of propionyl-CoA below that of acetyl-CoA, which means that the specificity for propionate uptake and activation to the corresponding CoA-ester is different to that from *A. nidulans*. This is also substituted by the different activities of acyl-CoA synthetase from both organisms. *A. nidulans* and *A. fumigatus* posses at least two enzymes capable for the activation of acetate and propionate, one having a higher specificity for acetate and the other for propionate. The remarkable difference is that the overall activity for activation of acetate is always higher in *A. nidulans* than that for the activation of propionate (Table 5). In *A. fumigatus* propionyl-CoA synthetase activity exceeds that of acetyl-CoA synthetase, especially when only propionate and no acetate is present. This result gives a possible explanation, why *A. fumigatus* generally reacts more sensitive towards the addition of propionate than *A. nidulans*. However, in order to elucidate the specific activity of the single enzymes and their impact on acetate and propionate activation, mutants have to be created, which posses only one of the two genes.

Investigations on the conidial surface revealed the existence of a link between spore colour, which is equivalent to the polyketides present, and the highly ordered protein layer surrounding the surface of conidia. The loss of pigmentation in the presence of propionate coincides with a loss of surface proteins. The observation that whitish conidia of a methylcitrate synthase mutant were stronger attenuated in the larval infection model than green spores implies that a wild-type surface is important in fending off the immune attack of the host. Whether this is also true in a murine infection model remains to be proven, but the fact that the whitish spores behaved like a *pks*P mutant is a good implication.

However, not only the loss of spore surface proteins seems to be important for an attenuation of virulence of the methylcitrate synthase mutants, but also the absence of methylcitrate synthase itself. As insects generally contain large amounts of proteins we can assume that a germinated *A. fumigatus* spore will use these proteins as carbon source. In that case, the amino acids isoleucine, valine and methionine become degraded, which yields propionyl-CoA that accumulates in the mutant strain. Due to the strong inhibition of the pyruvate dehydrogenase complex by propionyl-CoA a slow-down of energy metabolism will occur, which enables the larvae to overcome the infection. Whether amino acids are also a carbon source during infection of mammals needs to be proven.

In order to gain further insights into the impact of methylcitrate synthase on establishment of an invasive aspergillosis, further experiments will have to be performed. Therefore, we plan to investigate the survival rate of conidia from the methylcitrate synthase mutant in alveolar macrophages in comparison to the wild type and a *pksP* mutant and to test the attenuation of virulence in a murine model. These experiments will help to evaluate, whether the methylcitrate cycle is a suitable target for drug development against invasive aspergillosis or fungal infections in general.

Experimental procedures

Growth conditions and purification of methylcitrate synthase from *A. fumigatus*

Conidia of strain ATCC46645 were produced on 2% agar plates containing glucose as carbon source. For purification of methylcitrate synthase 3 L of liquid minimal medium in a 5 L flask containing 50 mM sodium propionate were inoculated with 2×10^6 conidia·mL^{-1} and incubated at 37 °C for 6 days under vigorous shaking (220 r.p.m). Mycelium was harvested by filtration over Miracloth filter gaze (Merk, Schwalbach/Ts, Germany) pressed dry and frozen in liquid nitrogen. Mycelium was ground to a fine powder, suspended in buffer A (50 mM Tris/HCl, pH 8.0) and centrifuged at 22 000 ***g*** for 25 min at 4 °C in a centrifuge (Sorvall RC-5B). The clear supernatant was saturated with solid ammonium sulphate to 50% and precipitated proteins were removed by centrifugation at 4 °C for 10 min and 15 000 ***g***. The supernatant was saturated to 90% and precipitated proteins were collected by centrifugation and solved in a minimal volume of buffer A. A Phenyl Sepharose column (bed volume 25 mL, Amersham Biosciences, Freiburg, Germany), previously equilibrated with buffer B [50 mM Tris/HCl, pH 8.0 containing 1 M $(NH_4)_2SO_4$] was loaded and proteins were eluted with a gradient from 100% buffer B to 100% buffer A. Fractions were tested for methylcitrate synthase activity, combined and dialysed against 5 L of buffer C (20 mM potassium phosphate pH 7.0). A hydroxyapatite column (bed volume 10 mL, Fluka, Taufkirchen, Germany) was equilibrated with buffer C and the dialysed enzyme pool was loaded. Proteins were eluted with an increasing potassium phosphate gradient against buffer D (350 mM potassium phosphate, pH 7.0). Fractions were tested for activity and combined. The pool was desalted by concentration and dilution by use of an amicon chamber equipped with a filter with a 30 kDa cut-off (Millipore, Schwalbach, Germany). Protein concentrations were determined by the BCA-Test (Pierce Biotechnology, Rockford, IL, USA) following the manufacturer's protocol and use of bovine serum albumin as a standard.

Biochemical characterization of *A. fumigatus* methylcitrate synthase

Methylcitrate synthase and citrate synthase activities were assayed with propionyl-CoA (0.2 mM) or acetyl-CoA (0.2 mM) in a condensing reaction with oxaloacetate (1 mM) as described earlier [5]. One unit of activity was defined as the release of 1 μmol CoASH per min.

Temperature dependence of methylcitrate synthase activity was measured in the standard assay in a range of 20 °C to 75 °C. Temperature stability was checked by incubating the enzyme for different times at several temperatures and determination of the residual activity in comparison to a sample incubated on ice. The pH dependence of activity was measured by replacing the Tris/HCl (pH 8.0) buffer used in the standard assay against a buffer combination containing 0.1 M boric acid, 0.1 M acetic acid, 0.1 M phosphoric acid; pH adjusted from 5.5 to 10.5 with 10 M NaOH. Substrate concentrations were kept as described above. The pH stability was determined by diluting the enzyme in the combined buffer system at different pH values. The time dependent decrease of enzymatic activity was determined under standard assay conditions.

K_m values for the substrates oxaloacetate, acetyl-CoA and propionyl-CoA were determined by measuring the release of CoASH in dependence of the concentration of one substrate, whereas that of the other was kept constant (0.2 mM for CoA-esters and 1 mM for oxaloacetate).

Inhibition of the pyruvate dehydrogenase complex by propionyl-CoA and excretion of pyruvate to the growth medium

The activity of the pyruvate dehydrogenase complex (PDH complex) was measured as described in [3]. Glucose grown mycelium was taken as a source for the PDH complex. The K_m value for CoASH was defined by use of different CoASH concentrations in the range of 0.19 and 0.019 mM. The K_i for propionyl-CoA was determined in the presence of 0.15 mM propionyl-CoA and varying concentrations of CoASH.

Pyruvate excretion to the medium after growth of different strains on different carbon sources was tested by the conversion of pyruvate to lactate by use of lactate dehydrogenase from rabbit muscle (Roche Diagnostics, Mannheim, Germany) as described in [3].

Determination of acyl-CoA synthetase activity and preparation of intracellular acyl-CoA

Acetyl-CoA and propionyl-CoA synthetase activity was determined from crude extracts of *A. fumigatus* ATCC46645 grown on various C-sources. Both activities were defined in a coupled assay with malate dehydrogenase and citrate synthase or methylcitrate synthase, respectively, as described earlier [3]. K_m values for the substrates acetate and propionate were determined by variation of the substrate concentration in a range of 2 mM and 0.05 mM.

Intracellular acetyl-CoA and propionyl-CoA levels were measured as described in [8]. In brief, lyophilized mycelium was ground to a fine powder and acyl-CoA was extracted under acid conditions. Partial purification was performed by the use of C18 cartridges and the amount of each CoA-ester was determined by use of citrate synthase and methylcitrate synthase, respectively.

Gel electrophoresis, blotting and N-terminal sequence identification

For analysis of protein fractions obtained from the purification of methylcitrate synthase, SDS/PAGE was carried out by use of a 15% polyacrylamide gel [35]. For N-terminal sequencing the protein was blotted from a 10% polyacrylamide gel on a polyvinylidene difluoride membrane (PVDF) with a transblot SD semi dry electrophoretic transfer cell (Bio-Rad Laboratories, Munich, Germany) as described in the manufacturer's protocol. N-terminal sequencing was kindly performed by D. Linder (Justus-Liebig-University Giessen, Germany) as described elsewhere [36].

Growth inhibition and field emission scanning microscopy (FESEM)

Growth inhibition was determined from liquid cultures in minimal medium. Carbon sources were 50 mM glucose, 50 mM sodium acetate and varying concentrations of sodium propionate in a range of 10–50 mM. Media (100 mL each in replicates) were inoculated with 5×10^5 conidia·mL^{-1} (final concentration) and incubated at 37 °C and 220 r.p.m. shaking for indicated times. Mycelia were harvested and dried for at least 12 h at 70 °C. Dried mycelium was weighed and growth inhibition was calculated in reference to mycelial weight from control cultures.

For preparation of spore suspensions for scanning field emission microscopy solid media containing 50 mM glucose with and without 10 mM propionate, respectively, were used. Plates were point inoculated with conidia from strains ATCC46645 (wild type), *ΔmcsA* and *pksP* mutants, respectively, and agar plates were incubated for 6 days at 37 °C. Conidia were harvested with water containing 10 mM $MgCl_2$ and 10 mM $CaCl_2$ and filtered over a 40 μm cell strainer (BD Bioscience, Heidelberg, Germany). Total spore concentrations were determined and conidia were collected by centrifugation. Conidia were resuspended in 10 mM $MgCl_2$ and 10 mM $CaCl_2$ to give a final concentration of 3×10^8 conidia·mL^{-1}.

Conidia were fixed with a fixation solution containing 5% (v/v) formaldehyde and 2% (v/v) glutaraldehyde in cacodylate buffer (0.1 M cacodylate, 0.01 M $CaCl_2$, 0.01 M $MgCl_2$, 0.09 M sucrose, pH 6.9) and washed first with cacodylate buffer then with TE buffer (10 mM Tris/HCl, 2 mM EDTA, pH 6.9). Samples were then placed onto poly(L-lysine) coated glass cover slips, allowed to settle down for 5 min and subsequently fixed with 3% (v/v) glutaraldehyde in TE buffer for 15 min at room temperature. After two washing steps with TE buffer samples were dehydrated with a graded series of acetone (10, 30, 50, 70, 90, 100%) on ice for 30 min for each step. Samples in the 100% acetone step were allowed to reach room temperature before another change of 100% acetone. Samples were then subjected to critical point drying with liquid CO_2 (CPD030, Balzers, Liechtenstein). The dried samples were covered with an approximately 10 nm thick gold film by sputter coating (SCD040, Balzers Union, Liechtenstein) before examination in a field emission scanning electron microscope Zeiss DSM 982 Gemini using the Everhart Thornley SE detector and the inlens detector in a 50 : 50 ratio at an acceleration voltage of 5 kV. Data were stored digitally on MO disks.

Test on H_2O_2 sensitivity

Conidia from wild-type ATCC46645, methylcitrate synthase deletion strain (*ΔmcsA*) and polyketide synthase (*pksP*$^-$) mutant were harvested from glucose and glucose/propionate (10 mM) minimal medium, respectively. Conidia were washed once with 0.1% Tween 80 + 0.9% NaCl (to separate spores) and resuspended in water to give a final concentration of 3×10^8 conidia·mL^{-1}. Bottom agar (65 mL) consisting of glucose minimal medium with 2% agar was poured into a Petri dish (diameter of 13.5 cm) and cooled to about 35 °C. Top agar (24 mL with same composition as bottom agar) was mixed with 1 mL of spore suspension and poured on top of the bottom agar. Three holes with a diameter of 1 cm were punched into each agar plate and different amounts of a 3% H_2O_2 solution were applied. Plates were incubated for 20 h at 37 °C and inhibition zones were determined as an average of three samples each.

Effect of co-metabolism of amino acids on polyketide synthesis

The amino acids methionine, valine and isoleucine were used as sources of propionyl-CoA, whereas glutamate was used as a control. Glucose and nitrate containing agar plates were supplemented with 25 mM (final concentration) of each L-amino acid. The wild-type strain ATCC46645 and a methylcitrate synthase deletion strain were point inoculated on each plate and incubated for 72 h at 37 °C and photographed.

Synthesis of cDNA and sequence analysis

Propionate grown cultures of *A. fumigatus* ATCC46645 were used for preparation of RNA. Total RNA was isolated by use of the Plant DNeasy Miniprep Kit (Qiagen, Hilden, Germany) as described in the manufacturer's protocol. cDNA was amplified in a one-tube reaction using the RobusT I RT-PCR Kit (BioCat, Heidelberg, Germany) and sequence specific oligonucleotides cDNAmcsAAf_up and cDNAmcsAAf_down (Table 8). PCR products were cloned into the pDrive cloning vector (Qiagen) and transferred into *E. coli* XL1-blue MRF′ (MBI Fermentas, St. Leon-Rot, Germany). Plasmid DNA was reisolated by standard methods and sequenced from both strands by SeqLab (Göttingen, Germany). The resulting sequence was aligned against the genomic DNA derived from the *A. fumigatus*

Table 8. Oligonucleotides used in this study. Half and full *Not*I restriction sites are shown in bold.

Name of oligonucleotide	Sequence 5′ → 3′
cDNAmcsAAf_up	GAC CAT CCC TTG ATA GCA TC
cDNAmcsAAf_down	GAT ATC ACA GGC TCA CAG G
NotMcsAAf_up	**CCG C**CT TCA GAG CGG TCT TG
NotMcsAAf_down	**CCG C**CT CCG GAG TCC TCT TC
AfumMcsAup	GGC CTG AGG CGA TTC AGG G
AfumMcsAdown	CGC TCG CTA CAC TCC TCT CG
NotPyrGAn_up	**GCG GCC GC**T TCG TTA AGG ATA ATT GC
NotPyrGAn_down	**GCG GCC GC**A ATA AAC ATA TGG ATC C

genome-sequencing project (http://www.tigrblast.tigr.org/ufmg/). The protein sequence was obtained by use of the translate tool from the Expasy home page (http://www.expasy.org/). Further analysis of the sequence was performed with the programs PSORT (http://www.psort.nibb.ac.jp/form2.html) MITOPROT (http://www.ihg.gsf.de/ihg/mitoprot.html) and PROTPARAM (http://www.expasy.org/tools/protparam.html), which can all be found at the Expasy home page.

Deletion of the methylcitrate synthase gene

As a parental strain for gene deletion the uracil auxotrophic strain CEA17 was used, which contains a point mutation in the *pyrG* locus [37]. As a selectable marker the *pyrG* gene from *A. nidulans* was used. The *mcsA* gene including 1000 bp upstream and downstream flanking regions was amplified from genomic DNA of the wild-type strain ATCC46645 by use of the oligonucleotides McsAAf_up and McsAAF_down (Table 8). The PCR product was cloned into the PCR2.1 vector (Invitrogen, Karlsruhe, Germany) and transferred into *E. coli* TOP10 cells (Invitrogen). Plasmid DNA was purified by standard methods and restricted with *Eco*RI to release the PCR-product from the vector. The restriction fragment was subcloned into pUC18 (MBI Fermentas) and used as a template in a PCR reaction. The proofreading Accuzyme DNA polymerase (Bioline, Luckenwalde, Germany) and the 5′-phosphorylated oligonucleotides NotMcsAAf_up (which reads towards the 5′- upstream region) and NotMcsAAF_down (which reads towards the 3′-downstream region) were used. Both oligonucleotides contained a half *Not*I restriction site at their 5′-end. The resulting PCR product contained the sequence of the pUC18 vector including the up- and downstream region but excluded 80% of the coding region of the methylcitrate synthase. Blunt end ligation of the product introduced a new *Not*I restriction site and enabled subcloning of a *Not*I restricted *pyrG* gene from *A. nidulans* between the up- and downstream region, yielding a pUC18 vector, which contained the deletion construct (pUCΔmcsAAfPyrG). The *pyrG* gene was amplified from genomic DNA of an *A. nidulans* wild-type strain (A26, fungal genetics stock centre, Kansas, USA) by use of the oligonucleotides NotPyrGAn_up and NotPyrGAn_down and subcloned into the PCR2.1 vector (Invitrogen).

Plasmid pUCΔmcsAAfPyrG was restricted with *Eco*RI in order to remove the pUC18 vector backbone. After gel purification (QIAquick Gel Extraction kit, Qiagen) the deletion part was directly used for transformation of *A. fumigatus* CEA17 by a method described earlier [37].

Transformants were prescreened for their ability to use propionate as sole carbon and energy source, followed by Southern blot analysis of *Eco*RV restricted genomic DNA. Probes against the *pyrG* gene from *A. nidulans* and against the *mcsA* gene from *A. fumigatus* were labelled with digoxigenin. For detection of DNA-fragments anti-digoxigenin Fab-fragments linked to alkaline phosphatase (Roche Diagnostics) were used.

Virulence studies in an insect infection model using larvae of *Galleria mellonella*

Conidia for the infection of larvae were harvested in phosphate buffered saline ($NaCl/P_i$) and filtered through a cell strainer. Spore suspensions were concentrated to 5×10^8 conidia·mL^{-1} by centrifugation and resuspension in $NaCl/P_i$ containing 10 μg rifampicin·mL^{-1} to avoid bacterial infections. Each larvae with a weight of around 0.2 g was infected with 10 μL of spore suspension through the last left proleg and incubated for 6 days at 21 °C to 23 °C in the dark. Controls were inoculated with 10 μL of $NaCl/P_i$/rifampicin. Survival was monitored every 12 h by checking to movement of the larvae.

Acknowledgements

This work was supported by a grant of the Deutsche Forschungsgemeinschaft (project BR 2216). Judith Behnsen and Yvonne Speidel are gratefully acknowledged for their help in establishing the plate diffusion assays and the *Galleria mellonella* infection model, respectively.

References

1 Conrad R & Klose M (1999) Anaerobic conversion of carbon dioxide to methane, acetate and propionate on washed rice roots. *FEMS Microbiol Ecol* **30**, 147–155.
2 Ledley FD, Crane AM, Klish KT & May GS (1991) Is there methylmalonyl CoA mutase in *Aspergillus nidulans*. *Biochem Biophys Res Commun* **177**, 1076–1081.
3 Brock M & Buckel W (2004) On the mechanism of action of the antifungal agent propionate. *Eur J Biochem* **271**, 3227–3241.
4 Brock M, Darley D, Textor S & Buckel W (2001) 2-Methylisocitrate lyases from the bacterium *Escherichia*

coli and the filamentous fungus *Aspergillus nidulans*: characterization and comparison of both enzymes. *Eur J Biochem* **268**, 3577–3586.
5 Brock M, Fischer R, Linder D & Buckel W (2000) Methylcitrate synthase from *Aspergillus nidulans*: implications for propionate as an antifungal agent. *Mol Microbiol* **35**, 961–973.
6 Maruyama K & Kitamura H (1985) Mechanisms of growth inhibition by propionate and restoration of the growth by sodium bicarbonate or acetate in *Rhodopseudomonas sphaeroides* S. *J Biochem (Tokyo)* **98**, 819–824.
7 Brass EP & Beyerinck RA (1988) Effects of propionate and carnitine on the hepatic oxidation of short- and medium-chain-length fatty acids. *Biochem J* **250**, 819–825.
8 Zhang YQ, Brock M & Keller NP (2004) Connection of propionyl-CoA metabolism to polyketide biosynthesis in *Aspergillus nidulans*. *Genetics* **168**, 785–794.
9 Zhang YQ & Keller NP (2004) Blockage of methylcitrate cycle inhibits polyketide production in *Aspergillus nidulans*. *Mol Microbiol* **52**, 541–550.
10 Denning DW (1998) Invasive asperillosis. *Clin Infect Dis* **26**, 781–803.
11 Denning DW (2000) Early diagnosis of invasive aspergillosis. *Lancet* **355**, 423–424.
12 Latgé JP (1999) *Aspergillus fumigatus* and aspergillosis. *Clint Microbiol Rev* **12**, 310–350.
13 Brakhage AA & Langfelder K (2002) Menacing mold: the molecular biology of *Aspergillus fumigatus*. *Annu Rev Microbiol* **56**, 433–455.
14 Schrettl M, Bignell E, Kragl C, Joechl C, Rogers T, Arst HN Jr, Haynes K & Haas H (2004) Siderophore biosynthesis but not reductive iron assimilation is essential for *Aspergillus fumigatus* virulence. *J Exp Med* **200**, 1213–1219.
15 Liebmann B, Muller M, Braun A & Brakhage AA (2004) The cyclic AMP-dependent protein kinase a network regulates development and virulence in *Aspergillus fumigatus*. *Infect Immun* **72**, 5193–5203.
16 Liebmann B, Muehleisen TW, Mueller M, Hecht M, Weidner G, Braun A, Brock M & Brakhage AA (2004) Deletion of the *Aspergillus fumigatus* lysine biosynthesis gene *lysF* encoding homoaconitase leads to attenuated virulence in a low-dose mouse infection model of invasive aspergillosis. *Arch Microbiol* **181**, 378–383.
17 Krappmann S, Bignell EM, Reichard U, Rogers T, Haynes K & Braus GH (2004) The *Aspergillus fumigatus* transcriptional activator CpcA contributes significantly to the virulence of this fungal pathogen. *Mol Microbiol* **52**, 785–799.
18 Jahn B, Koch A, Schmidt A, Wanner G, Gehringer H, Bhakdi S & Brakhage AA (1997) Isolation and characterization of a pigmentless-conidium mutant of *Aspergillus fumigatus* with altered conidial surface and reduced virulence. *Infect Immun* **65**, 5110–5117.
19 Langfelder K, Jahn B, Gehringer H, Schmidt A, Wanner G & Brakhage AA (1998) Identification of a polyketide synthase gene (*pksP*) of *Aspergillus fumigatus* involved in conidial pigment biosynthesis and virulence. *Med Microbiol Immunol* **187**, 79–89.
20 Jahn B, Langfelder K, Schneider U, Schindel C & Brakhage AA (2002) PKSP-dependent reduction of phagolysosome fusion and intracellular kill of *Aspergillus fumigatus* conidia by human monocyte-derived macrophages. *Cell Microbiol* **4**, 793–803.
21 Langfelder K, Philippe B, Jahn B, Large JP & Brakhage AA (2001) Differential expression of the *Aspergillus fumigatus pksP* gene detected *in vitro* and *in vivo* with green fluorescent protein. *Infect Immun* **69**, 6411–6418.
22 Jahn B, Boukhallouk F, Lotz J, Langfelder K, Wanner G & Brakhage AA (2000) Interaction of human phagocytes with pigmentless *Aspergillus* conidia. *Infect Immun* **68**, 3736–3739.
23 Paris S, Debeaupuis JP, Crameri R, Carey M, Charles F, Prevost MC, Schmitt C, Philippe B & Latgé JP (2003) Conidial hydrophobins of *Aspergillus fumigatus*. *Appl Environ Microbiol* **69**, 1581–1588.
24 Payton MA, McCullough W, Roberts CF & Guest JR (1977) Two unlinked genes for the pyruvate dehydrogenase complex in *Aspergillus nidulans*. *J Bacteriol* **129**, 1222–1226.
25 Schrenk DF & Bisswanger H (1984) Measurements of electron spin resonance with the pyruvate dehydrogenase complex from *Escherichia coli*. Studies on the allosteric binding site of acetyl-coenzyme A. *Eur J Biochem* **143**, 561–566.
26 Watanabe A, Fujii I, Sankawa U, Mayorga ME, Timberlake WE & Ebizuka Y (1999) Re-identification of *Aspergillus nidulans wA*-gene for a polyketide synthase of naphthopyrone. *Tetrahedron Lett* **40**, 91–94.
27 Thau N, Monod M, Crestani B, Rolland C, Tronchin G, Latgé JP & Paris S (1994) rodletless mutants of *Aspergillus fumigatus*. *Infect Immun* **62**, 4380–4388.
28 Girardin H, Paris S, Rault J, Bellon-Fontaine MN & Large JP (1999) The role of the rodlet structure on the physicochemical properties of *Aspergillus* conidia. *Lett Appl Microbiol* **29**, 364–369.
29 Jander G, Rahme LG & Ausubel FM (2000) Positive correlation between virulence of *Pseudomonas aeruginosa* mutants in mice and insects. *J Bacteriol* **182**, 3843–3845.
30 Cotter G, Doyle S & Kavanagh K (2000) Development of an insect model for the in vivo pathogenicity testing of yeasts. *FEMS Immunol Med Microbiol* **27**, 163–169.
31 Brennan M, Thomas DY, Whiteway M & Kavanagh K (2002) Correlation between virulence of *Candida albicans* mutants in mice and *Galleria mellonella* larvae. *FEMS Immunol Med Microbiol* **34**, 153–157.
32 Dunphy GB, Oberholzer U, Whiteway M, Zakarian RJ & Boomer I (2003) Virulence of *Candida albicans*

mutants toward larval *Galleria mellonella* (*Insecta*, *Lepidoptera*, *Galleridae*). *Can J Microbiol* **49**, 514–524.
33 Bergin D, Brennan M & Kavanagh K (2003) Fluctuations in haemocyte density and microbial load may be used as indicators of fungal pathogenicity in larvae of *Galleria mellonella*. *Microbes Infect* **5**, 1389–1395.
34 Reeves EP, Messina CG, Doyle S & Kavanagh K (2004) Correlation between gliotoxin production and virulence of *Aspergillus fumigatus*. *Galleria mellonella*. *Mycopathologia* **158**, 73–79.
35 Laemmli U.K. (1970) Cleavage of structural protein during assembly of the head of bacteriophage T4. *Nature* **227**, 680–685.
36 Michel C, Hartrampf G & Buckel W (1989) Assay and purification of the adenosylcobalamin-dependent 2-methyleneglutarate mutase from *Clostridium barkeri*. *Eur J Biochem* **184**, 103–107.
37 Weidner G, d'Enfert C, Koch A, Mol PC & Brakhage AA (1998) Development of a homologous transformation system for the human pathogenic fungus *Aspergillus fumigatus* based on the *pyrG* gene encoding orotidine 5′-monophosphate decarboxylase. *Curr Genet* **33**, 378–385.